

Something something something physics

Steven Green
of Emmanuel College

A dissertation submitted to the University of Cambridge
for the degree of Doctor of Philosophy

Abstract

LHCb is a b-physics detector experiment which will take data at the 14 TeV LHC accelerator at CERN from 2007 onward...

Declaration

This dissertation is the result of my own work, except where explicit reference is made to the work of others, and has not been submitted for another qualification to this or any other university. This dissertation does not exceed the word limit for the respective Degree Committee.

Andy Buckley

Acknowledgements

Of the many people who deserve thanks, some are particularly prominent, such as my supervisor...

Preface

This thesis describes my research on various aspects of the LHCb particle physics program, centred around the LHCb detector and LHC accelerator at CERN in Geneva.

For this example, I'll just mention Chapter ?? and Chapter ??.

Contents

1. The Sensitivity of CLIC to Anomalous Gauge Couplings through Vector Boson Scattering	1
1.1. Background	1
1.2. Event Generation	2
1.3. Validation of New Samples	3
1.4. Simulation and Reconstruction	6
1.5. Analysis Processor and Jet Pairing	6
1.6. Methodology for Fitting	11
1.7. Optimisation of Jet Reconstruction	11
1.8. Event Selection	11
1.8.1. Pre Selection	16
1.8.2. MVA	16
1.9. Fit	16
A. Pointless extras	17
A.1. Anomalous Gauge Coupling Quartic Vertices Of Relevance in Vector Boson Scattering	17
Bibliography	23
List of figures	25
List of tables	27

*“Writing in English is the most ingenious torture
ever devised for sins committed in previous lives.”*

— James Joyce

Chapter 1.

The Sensitivity of CLIC to Anomalous Gauge Couplings through Vector Boson Scattering

“Kids, you tried your best, and you failed miserably. The lesson is, never try.”

— Homer Simpson

1.1. Background

A process that will show sensitivity to the α_4 and α_5 anomalous gauge couplings in the CLIC experiment is vector boson scattering. There are several channels that will be affected by these anomalous couplings at CLIC and these are summarised in figures ??, ??, reffig:vbswz and ?? where $q = u, d, s, b, c$ and $l = e, \mu, \tau, \nu_e, \nu_\mu, \nu_\tau$.

To determine whether an event is sensitive to α_4 and α_5 it will be necessary to determine whether the visible final states have been produced from the decay of W and Z bosons. A key discriminator in this procedure will be the invariant mass of the W and Z candidates. In light of this the hadronic decays of the W and Z bosons are only considered as the leptonic decays may contain neutrinos.

As the W and Z bosons in vector boson scattering are intermediate states in the Feynman diagrams, they will not be directly observed in the detector and will instead

contribute to processes with the final states containing possible decay products of the bosons $\nu\nu qqqq$, $l\nu qqqq$ and $ll qqqq$. In theory all processes will be affected by non zero α_4 and α_5 , however, the effects may be extremely small as they contribute to very high order expansions of the Hamiltonian. Event generation software does not calculate the expansions of the Hamiltonian to all orders, but instead truncates the expansion to leave the dominant terms. In the case of anomalous couplings this corresponds to certain final state cross sections being invariant to changes in α_4 and α_5 .

1.2. Event Generation

The event generation software used by the CLIC experiment is Whizard [3,5]. Whizard version 1.97 was used for generating the new samples, while version 1.95 is used for the official CLIC samples. It was recommended by the Whizard authors to use version 1.97 as it contains a unitarisation scheme that ensures the probabilities remain physical up to high energies when considering the effect of anomalous gauge couplings.

It was necessary to specify the anomalous coupling model in Whizard to study their impact, however, this did enforce a unit CKM matrix. In the context of vector boson scattering this will restrict the decays of the W to $d\bar{u}$ and $s\bar{c}$, the W^+ to $u\bar{d}$ and $c\bar{s}$ and the Z to $u\bar{u}$, $d\bar{d}$, $s\bar{s}$, $c\bar{c}$, $b\bar{b}$. This has little overall impact on the study as the cross section calculation using this model was, within the errors quoted by Whizard, identical to the standard model CKM matrix. The only aspect of the analysis effected by this modification is flavour tagging of jets and this will be addressed in subsequent chapters.

To find out which states show sensitivity to the anomalous couplings two cross section calculations were made using different values of α_4 and α_5 for relevant processes involving the hadronic decays of the W and Z bosons from vector boson scattering, which can be found in table 1.1. In the standard model the values of α_4 and α_5 are zero. The only final states showing sensitivity to the anomalous couplings are $\nu\nu qqqq$, $l\nu qqqq$ and $ll qqqq$, which correspond to the final states from the Feynman diagrams shown above in figures ??, ??, `reffig:vbswz` and ??. As this analysis focuses on the hadronic decays of the bosons involved in vector boson scattering the final states involving leptonic decays of the bosons e.g. $\nu\nu llqq$ were not included in this cross check. These leptonic dominated final states were also removed from the background

samples used in this study as isolated lepton finding would largely veto all such events from selection.

The sensitivity of an individual event to the anomalous gauge couplings is determined through an event weight. This weight corresponds to the ratio using non-zero α_4 and α_5 and using zero α_4 and α_5 of the square of the matrix element used in the cross section calculation. This reweighting procedure has many advantages over the alternative procedure of generating new samples with fixed α_4 and α_5 most notably the absence of systematic errors that may appear in new event generation. Each event picks up different weights based on α_4 and α_5 as the matrix element contributions from the anomalous couplings depend upon the kinematics of the final state, which is unique for each event. Examples of the event weights as a function of α_4 and α_5 for selected events is shown in figure 1.4.

The cross check shows that the most sensitive channel to the anomalous gauge couplings is the $\nu\nu qqqq$ indicating that the best sensitivity measurement should focus upon this channel, which is the aim of this analysis.

The CLIC experiment has a repository of simulated and reconstructed samples that can be used for physics analyses, however, for the relevant final states there is no way to calculate the event weights for these samples. Therefore, new samples for which reweighting is possible were created and processed through the CLIC reconstruction chain. New samples were created only for the $\nu\nu qqqq$ final state as the $l\nu qqqq$ and $ll qqqq$ final states have a significantly lower sensitivity. As will be shown in subsequent chapters, the application of an isolated lepton finder in the selection processor will largely veto the $l\nu qqqq$ and $ll qqqq$ final states, therefore, the absence of weight information for these final states will not significantly affect the sensitivity measurement based on the $\nu\nu qqqq$ final state.

1.3. Validation of New Samples

An identical setup to that used for the official CLIC sample was used for the event generation and reconstruction. Several reconstructed level distributions were compared to the official CLIC samples and all were found to be comparably to each other. A selection of these distributions is shown in figures 1.2 and 1.3.

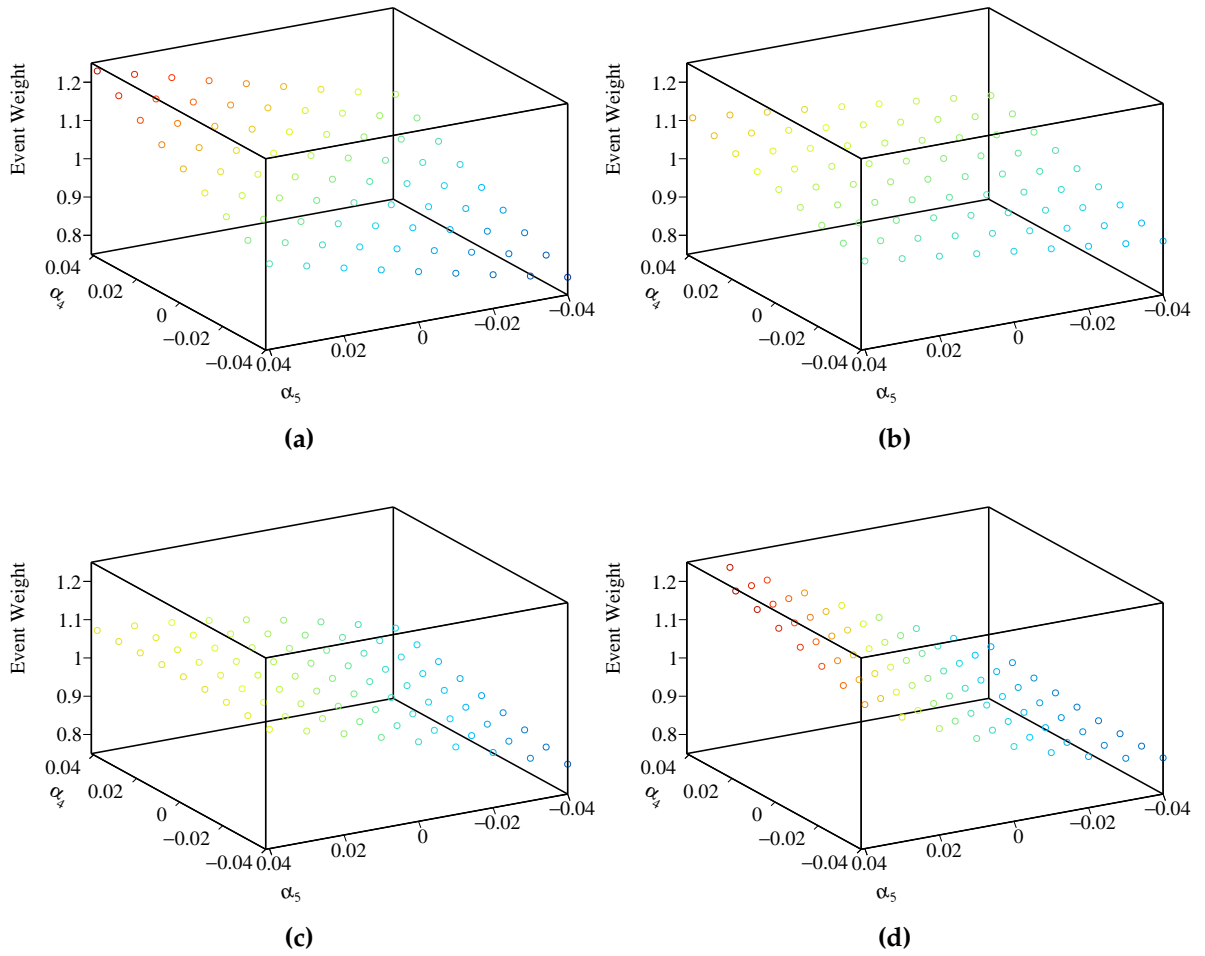


Figure 1.1.: A selection of plots showing how the event weight changes when varying the anomalous couplings α_4 and α_5 for 1.4 TeV $\nu\nu qq qq$ final state events.

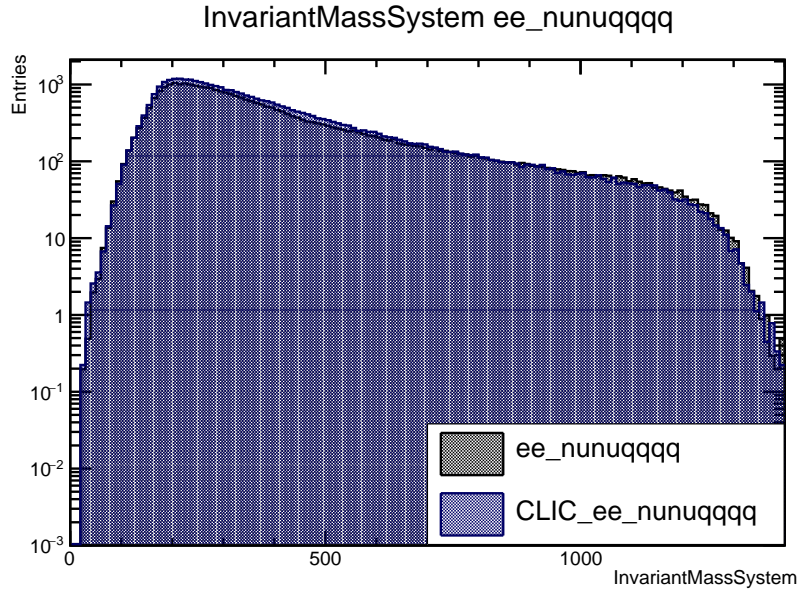


Figure 1.2.: Comparison between the invariant mass of the visible system for samples used in this analysis and the official CLIC samples for the $\nu\nu qq qq$ final state.

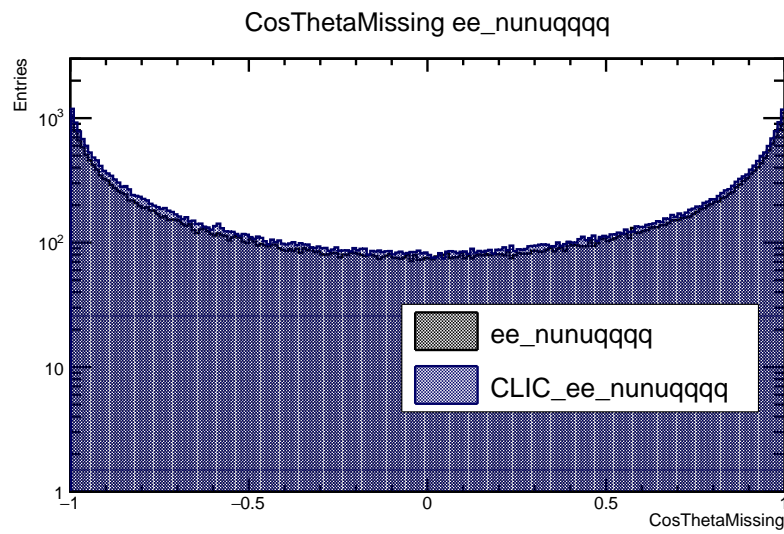


Figure 1.3.: Comparison between the $\cos\theta_{\text{Missing}}$ for samples used in this analysis and the official CLIC samples for the $\nu\nu qq qq$ final state.

Final State	Cross Section [fb] ($\alpha_4 = \alpha_5 = 0.00$)	Cross Section [fb] ($\alpha_4 = \alpha_5 = 0.05$)	Percentage Change[%]	CLIC Cross Section [fb]
$e^+e^- \rightarrow \nu\nu qqqq$	20.8	34.6	+66.3	24.7
$e^+e^- \rightarrow l\nu qqqq$	112	113	+0.9	115.3
$e^+e^- \rightarrow ll qqqq$	59.7	68.6	+14.9	71.7

Table 1.1.: Cross section for selected processes for given value of α_4 and α_5 . Channels considered where there were no changes to the cross section when varying α_4 and α_5 were $e^+e^- \rightarrow qqqq$, $e^+e^- \rightarrow \nu\nu qq$, $e^+e^- \rightarrow l\nu qq$, $e^+e^- \rightarrow ll qq$, $e^+e^- \rightarrow qq$, $\gamma_{EPA}e^- \rightarrow qqqqe^-$, $\gamma_{BS}e^- \rightarrow qqqqe^-$, $e^+\gamma_{EPA} \rightarrow qqqqe^+$, $e^+\gamma_{BS} \rightarrow qqqqe^+$, $\gamma_{EPA}e^- \rightarrow qqqq\nu$, $\gamma_{BS}e^- \rightarrow qqqq\nu$, $e^+\gamma_{EPA} \rightarrow qqqq\nu$, $e^+\gamma_{BS} \rightarrow qqqq\nu$, $\gamma_{EPA}\gamma_{EPA} \rightarrow qqqq$, $\gamma_{EPA}\gamma_{BS} \rightarrow qqqq$, $\gamma_{BS}\gamma_{EPA} \rightarrow qqqq$ and $\gamma_{BS}\gamma_{BS} \rightarrow qqqq$.

1.4. Simulation and Reconstruction

The CLIC_ILD detector [1] was simulated using the GEANT4 wrapper MOKKA and events were reconstructed using the MARLIN framework. Using the CLIC_ILD detector for this analysis provides access to the background samples created by the CLIC collaboration. The CLIC_ILD detector has a 60 layer scintillator-tugsten HCal in comparison to the 48 layer HCal found in the default ILD detector. The increase in thickness of the detector for the CLIC experiment is needed to compensate for the effects of leakage at the higher energies that will be seen by the CLIC experiment in comparison to the ILC. Practically speaking the ILD and CLIC_ILD detectors are otherwise identical.

Version of MOKKA used is 08-00-03. MarlinPandora version used is v00-09-02. PandoraPFANew version v00-09 [4,6].

1.5. Analysis Processor and Jet Pairing

For both signal and background events the FastJet processor is run to cluster the events into 4 jets. These are then assumed to be from the decays of the vector boson scattering bosons and the jets are paired up on the assumption that the correct pair arises when the invariant masses of the two pairs are closest together. The longitudinally invariant kt jet algorithm in exclusive modes is used for the jet clustering. This jet algorithm proceeds as follows:

- For each pair of particles i and j work out the k_t distance and beam distance $d_{iB} = p_t^2$.

$$d_{ij} = \min(p_{ti}^2, p_{tj}^2) \Delta R_{ij}^2 / R^2 \quad (1.1)$$

where $\Delta R_{ij}^2 = (y_i - y_j)^2 + (\phi_i - \phi_j)^2$. p_t is the transverse momentum of the particle with respect to the beam axis, y_i is the rapidity of particle i and ϕ_i is the azimuthal angle of particle i . R is a configurable parameter that typically is of the order of 1.

- Find the minimum distance d_{\min} of all the k_t and beam distances. If the minima occurs for a k_t distance, merge particles i and j , summing their 4-momenta in the energy combination scheme (also configurable). If the beam distance is the minimum declare particle i to be apart of the "beam" jet and remove it from the list of particles and not included in the final output jets.
- Repeat until no particles are left or the requested number of jets have been created (or optionally apply a minimum d_{cut} where clustering stops, but here the event is forced into 4 jets).

An inclusive mode is available, but not applied here as the finally number of jets in the output varies and events need to be clustered into 4 jets in this analysis. Two other clustering modes were considered, but were found to be inappropriate for this analysis as is shown in figure 1.4. They were:

- The k_t algorithm for e+e colliders (or Durham algorithm) where $d_{ij} = 2\min(E_i^2, E_j^2)(1 - \cos\theta_{ij})$ and d_{iB} is not used. θ_{ij} is the opening angle of the particles. In the collinear limit this corresponds to the relative transverse momentum of the particles. Unlike the other algorithm choices this is not invariant to boosts along the beam direction as in theory for e+e colliders the collision should occur with no net 3 momentum, unlike hadron colliders where the events have a net 3-momentum. However, the presence of ISR and beam effects makes this algorithm inappropriate for CLIC. The major failure of this algorithm choice is the absence of d_{iB} as this associates too many background particles to jets when applied at CLIC.
- The Cambridge/Aachen jet algorithm where $d_{ij} = \Delta R_{ij}^2 / R^2$ and $d_{iB} = 1$. This algorithm gave poor performance as it is based entirely on spacial information and does not account for the transverse momentum or energy of the particles being grouped. In essence this is a cone clustering algorithm with a cone radius

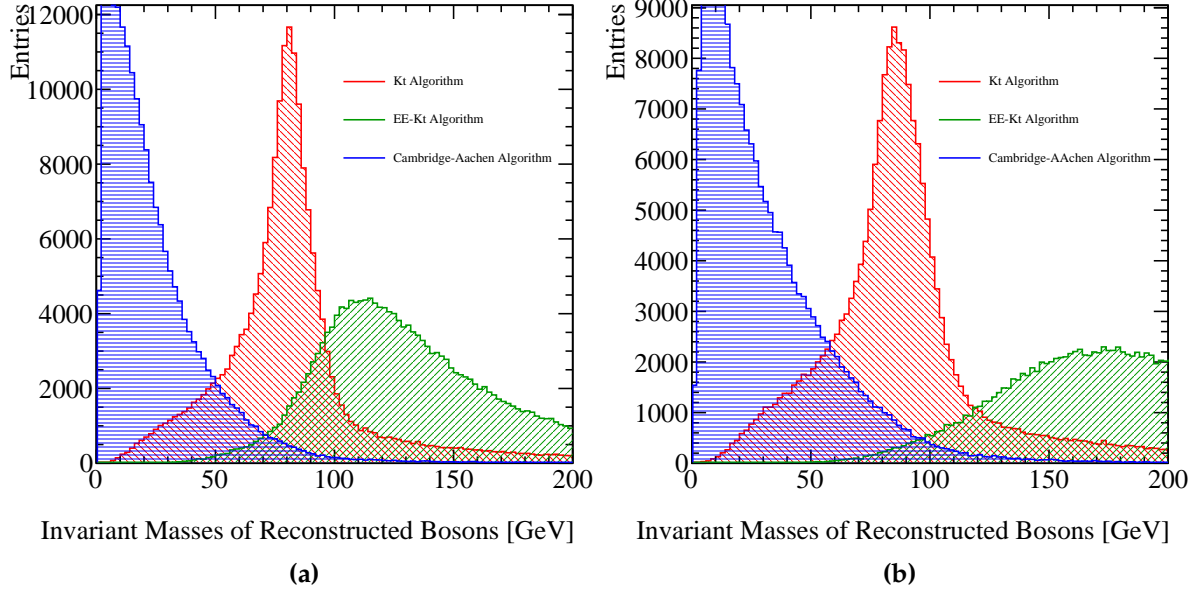


Figure 1.4.: Reconstructed masses for different choices of jet algorithm for 1.4 TeV and 3 TeV $\nu\nu q\bar{q}q\bar{q}$ events. These masses arise by forcing the reconstructed events into 4 jets and then pairing up the jets into pairs such that the reconstructed invariant masses of the pairs are closest to each other. These samples should be dominated by vector boson scattering involving pairs of W bosons and so it is expected that a peak at the W boson true mass should be observed. As this does not occur for the Cambridge-Aachen algorithm or the ee_kt algorithm they were deemed unsuitable for this analysis at both 1.4 and 3 TeV. In the case of the kt algorithm and the ee_kt algorithm an R parameter of 0.7 was used.

defined through $\Delta R_{ij} = R$, which even for large R was found to throw away too much energy in the event to be useful for this analysis. This algorithm can be useful for events with small jets that are highly boosted, but in this case the jets are too large to be successfully merged.

Alongside the jet clustering an isolated lepton finder is run to help reject background events containing high energy leptons. The LCFIPlus vertex processor is also run on these events once clustered into jets to produce a value for the B and C tag likelihood. This information is also used for background rejection instead of contributing to the sensitivity of the event to the anomalous couplings. The LCFIPlus vertex tagger was trained using events of $e^+e^- \rightarrow Z\nu\nu \rightarrow q\bar{q}\nu\nu$ for $q = u, d, s, c, b$.

Finally, an analysis processor is run, which calculates a number of variables used downstream in the analysis. Included in these are:

- Number of PFOs in the jets and the paired up bosons.
- Number of charged PFOs in the jets and paired up bosons.
- Highest energy PFO: energy, momentum, transverse momentum, $\cos\theta$.
- Highest energy electron PFO: energy, momentum, transverse momentum, $\cos\theta$.
- Highest energy muon PFO: energy, momentum, transverse momentum, $\cos\theta$.
- Highest energy photon PFO: energy, momentum, transverse momentum, $\cos\theta$.
- (If in existence) Highest and second highest energy isolated lepton: energy, momentum, transverse momentum, $\cos\theta$.
- Bosons: energy, momentum, transverse momentum, $\cos\theta$.
- Invariant mass of the boson pair.
- Jets: energy, momentum, transverse momentum, $\cos\theta$.
- $\cos\theta$ Of the missing 3-momentum vector.
- Recoil mass.
- Invariant mass of the visible system.
- y_i, y_{i+1} . Jet clustering parameters ranging from $i = 0$ to 6.
- $\cos\theta_{jet}^*$. This is the opening angle of a pair of jets, assumed to be from a single boson, in the rest frame of the boson.
- $\cos\theta_{Boson}^*$. This is the opening angle of a pair of bosons, assumed to be from vector boson scattering, in the rest frame of the di-boson pair.
- Transverse momentum and energy of the event.
- Acolinearity of the jet pairs forming the bosons and the acolinearity of the boson pair.
- Principle thrust T and the thrust axes $\bar{\mathbf{n}}$. Note $\bar{\mathbf{n}}$ is a unit vector. These are defined by the following equation

$$T = \max_{\bar{\mathbf{n}}} \left(\frac{\sum_i \mathbf{p}_i \cdot \bar{\mathbf{n}}}{\sum_i |\mathbf{p}_i|^2} \right) \quad (1.2)$$

- The major and minor thrust values. These are defined with respect to the thrust axes $\bar{\mathbf{n}}$ in the following way:

$$T = \max_{\bar{\mathbf{n}}_{major}} \left(\frac{\sum_i \mathbf{p}_i \cdot \bar{\mathbf{n}}_{major}}{\sum_i |\mathbf{p}_i|^2} \right) \quad (1.3)$$

where $\bar{\mathbf{n}}_{major} \cdot \bar{\mathbf{n}} = 0$. Similarly the minor thrust value is defined as

$$T = \frac{\sum_i \mathbf{p}_i \cdot \bar{\mathbf{n}}_{minor}}{\sum_i |\mathbf{p}_i|^2} \quad (1.4)$$

where $\bar{\mathbf{n}}_{minor} \cdot \bar{\mathbf{n}} = \bar{\mathbf{n}}_{minor} \cdot \bar{\mathbf{n}}_{major} = 0$

- Sphericity. This is defined using the sphericity tensor S^{ab} defined as:

$$S^{ab} = \frac{\sum_i p_i^a p_i^b}{\sum_{i,\alpha=1,2,3} |p_i^\alpha|^2} \quad (1.5)$$

Where p_i are the components of the momenta of particle i in the frame of the detector and the sum runs over all particles in the event. Sphericity is defined as $S = \frac{3}{2}(\lambda_2 + \lambda_3)$, where λ_i are the eigenvalues of the sphericity tensor defined such $\lambda_1 \geq \lambda_2 \geq \lambda_3$. This provides a measure of how spherical the reconstructed event topology is with isotropic events having $S \approx 1$, while two jet events have $S \approx 0$. (Also $\lambda_1 + \lambda_2 + \lambda_3 = 1$.)

- Aplanarity. Aplanarity is defined as $\frac{3}{2}\lambda_3$ where λ_3 is an eigenvalue of the sphericity tensor. This provides a measure of whether an event is linear or planar.
- B and C tag values for the jets, the min and max B and C tag values for the bosons.

Alongside these variables, for the $\nu\nu qqqq$ final state a number of Monte-Carlo variables are calculated for informative purposes and are not used in the analysis. These include:

- The quark and neutrino 4 momenta.
- Invariant mass of boson pair using MC pairing and MC energy.
- Invariant mass of boson pair using MC pairing and reconstructed jet energy.

1.6. Methodology for Fitting

It is necessary now to skip ahead to discuss the fitting procedure in this analysis as the optimisation of the jet algorithms relies on this methodology. In this section only the signal events are considered to determine the underlying sensitivity of the CLIC detector to the anomalous couplings. This decision was made to save analysis of the large number of background samples in the optimisation of the jet reconstruction algorithms, while still optimising the algorithm on the physics of interest.

The sensitivity of CLIC to the anomalous gauge couplings is determined through the use of a χ^2 fit to the distribution of $\cos\theta_{jets}^*$ where θ_{jets}^* is the angle between the two jets produced from the hadronic decay of the W/Z boson in the rest frame of that boson as done in BLAH.

1.7. Optimisation of Jet Reconstruction

1.8. Event Selection

As discussed earlier the signal events for this analysis contain the $\nu\nu qqqq$ final state. The processes to be considered in this analysis alongside the signal are events that would topologically look similar to signal in the detector. This includes events that could be confused with 4 jet events with missing energy, while excluding those events with large numbers of high energy leptons that could be vetoed easily during the analysis stage. In full the list includes:

Equivalent photon approximation processes models interactions of the electric field of the incoming electrons and positrons with their corresponding antiparticles at the collision point. In such interactions the electric fields of the charged particles are approximated as photons hence the name. The beamstrahlung processes model the collision of a photon radiated off a charged particle with the corresponding bunch incoming lepton. Photons are radiated from the incoming charged leptons as the bunches carrying the leptons are very small producing very large electromagnetic fields. Interactions with the charged leptons and these fields yields the beamstrahlung photons. The energy spectrum of the incoming particles for CLIC at the relevant

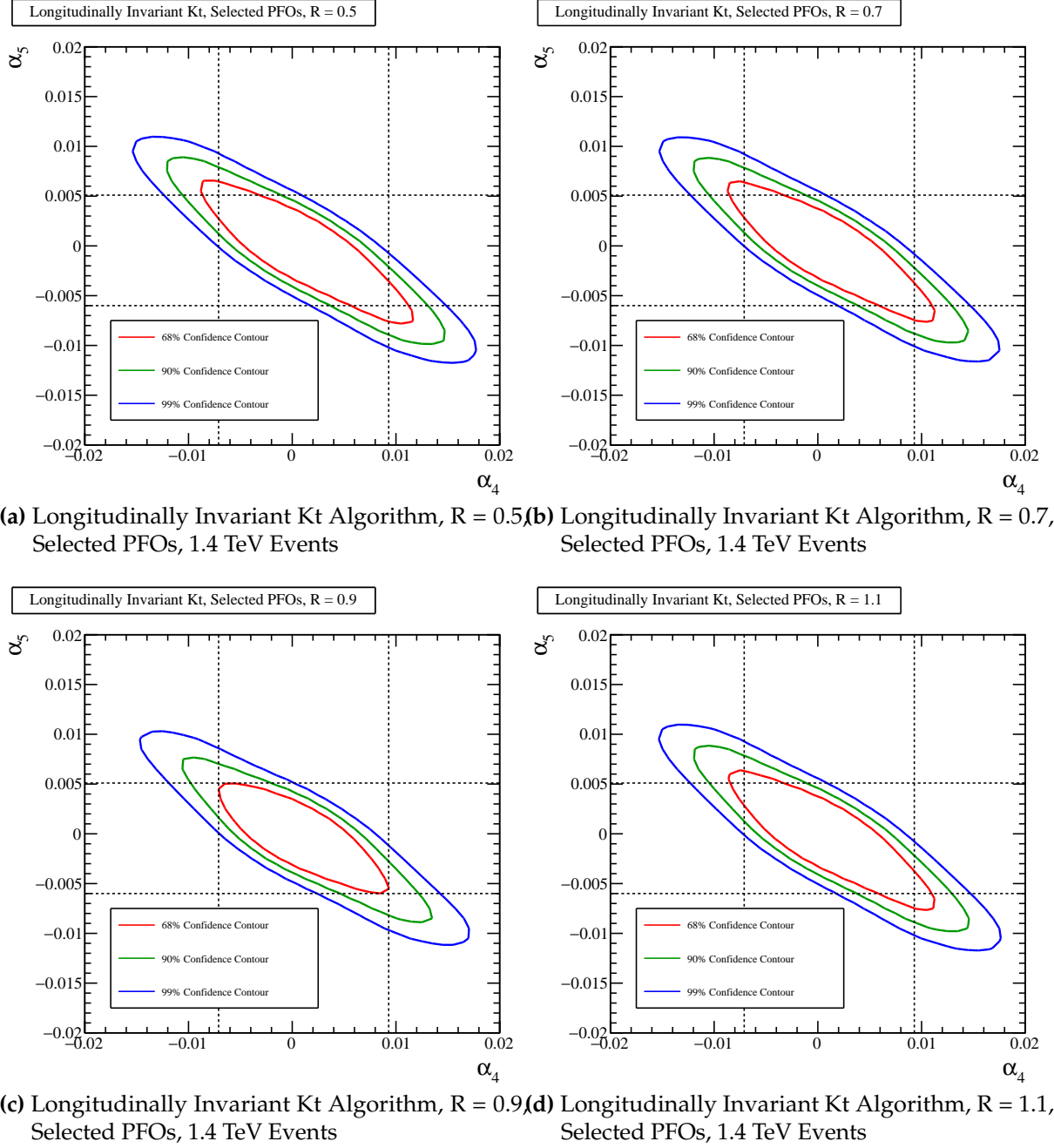
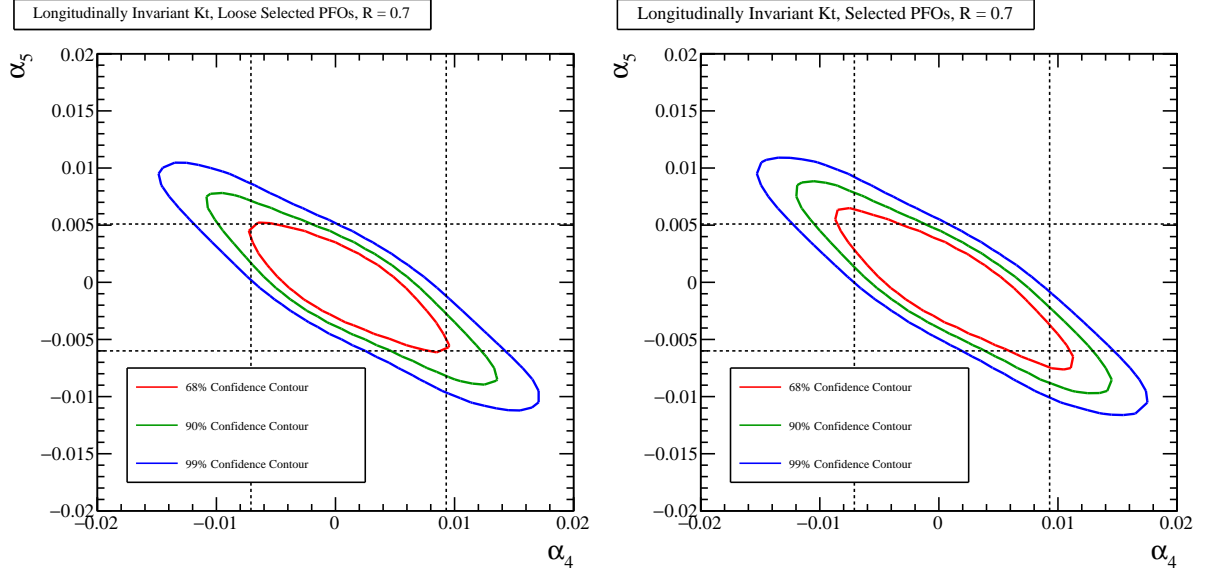
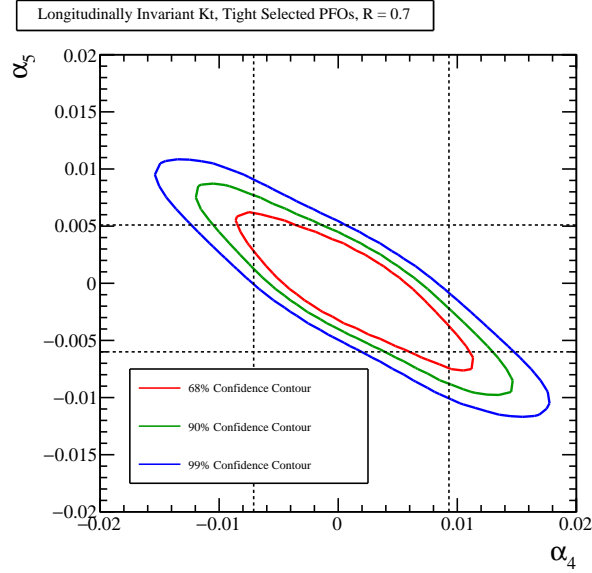


Figure 1.5.: χ^2 Sensitivity contours for the $qqqq\nu\nu$ final state arising from a fit to $\cos\theta_{\text{jets}}^*$ at 1.4 TeV for different values of the R parameter used in the jet reconstruction.



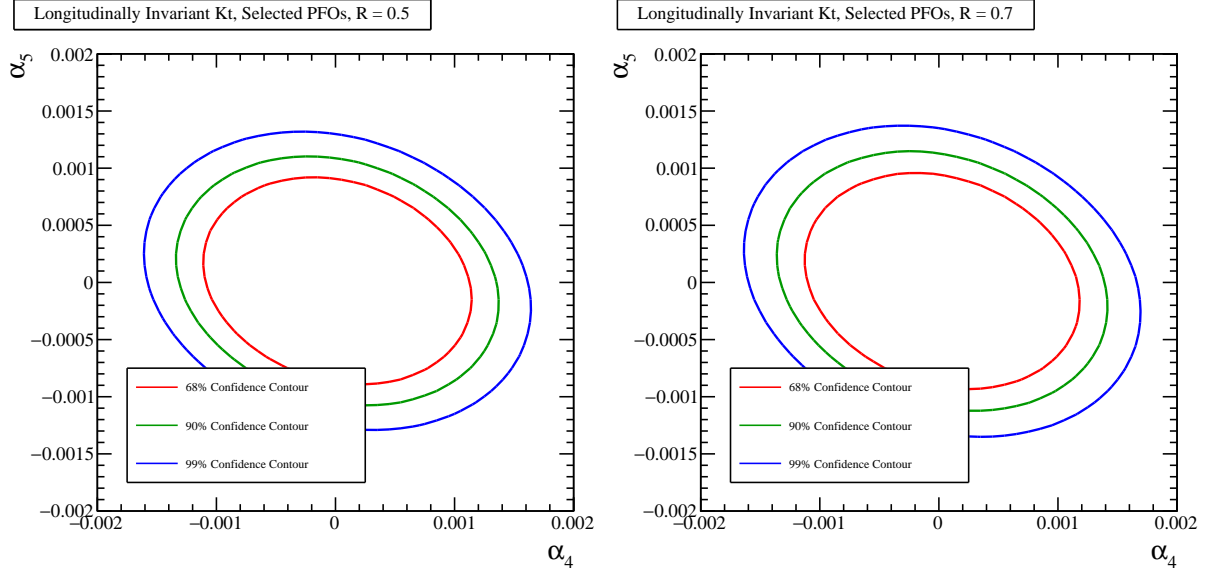
(a) Longitudinally Invariant Kt Algorithm, $R = 0.7$, Loose Selected PFOs, 1.4 TeV Events

(b) Longitudinally Invariant Kt Algorithm, $R = 0.7$, Selected PFOs, 1.4 TeV Events

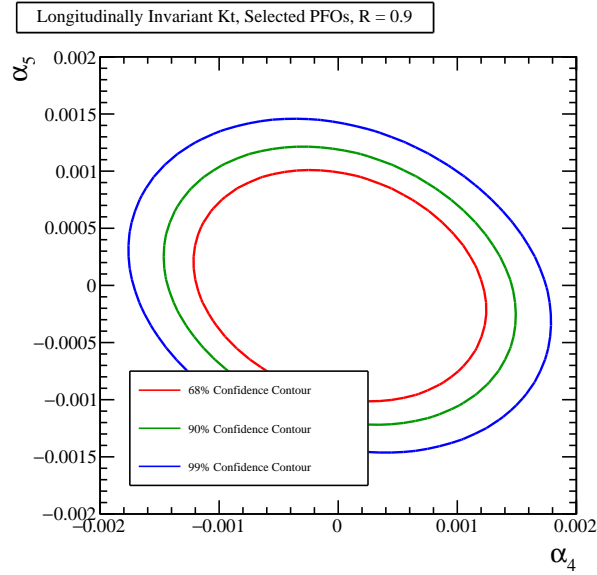


(c) Longitudinally Invariant Kt Algorithm, $R = 0.7$, Tight Selected PFOs, 1.4 TeV Events

Figure 1.6.: χ^2 Sensitivity contours for the $qq\bar{q}\bar{q}\nu\nu$ final state arising from a fit to $\cos\theta_{\text{jets}}^*$ at 1.4 TeV for different PFO selections.



(a) Longitudinally Invariant Kt Algorithm, $R = 0.5$, Selected PFOs, 3 TeV Events **(b)** Longitudinally Invariant Kt Algorithm, $R = 0.7$, Selected PFOs, 3 TeV Events



(c) Longitudinally Invariant Kt Algorithm, $R = 0.9$, Selected PFOs, 3 TeV Events

Final State	Cross Section 1.4 TeV [fb]	Cross Section 3 TeV [fb]
$e^+e^- \rightarrow \nu\nu qqqq$	24.7	71.5
$e^+e^- \rightarrow l\nu qqqq$	110.4	106.6
$e^+e^- \rightarrow ll qqqq$	62.1	169.3
$e^+e^- \rightarrow qqqq$	1245.1	546.5
$e^+e^- \rightarrow \nu\nu qq$	787.7	546.5
$e^+e^- \rightarrow l\nu qq$	4309.7	5560.9
$e^+e^- \rightarrow ll qq$	2725.8	3319.6
$e^+e^- \rightarrow qq$	4009.5	2948.9
$\gamma_{\text{EPA}}e^- \rightarrow qqqqe^-$	287.1	287.8
$\gamma_{\text{BS}}e^- \rightarrow qqqqe^-$	1160.7	1268.6
$e^+\gamma_{\text{EPA}} \rightarrow qqqqe^+$	286.9	287.8
$e^+\gamma_{\text{BS}} \rightarrow qqqqe^+$	1156.3	1267.3
$\gamma_{\text{EPA}}e^- \rightarrow qqqq\nu$	32.6	54.2
$\gamma_{\text{BS}}e^- \rightarrow qqqq\nu$	136.9	262.5
$e^+\gamma_{\text{EPA}} \rightarrow qqqq\nu$	32.6	54.2
$e^+\gamma_{\text{BS}} \rightarrow qqqq\nu$	136.4	262.3
$\gamma_{\text{EPA}}\gamma_{\text{EPA}} \rightarrow qqqq$	753.0	402.7
$\gamma_{\text{EPA}}\gamma_{\text{BS}} \rightarrow qqqq$	4034.8	2423.1
$\gamma_{\text{BS}}\gamma_{\text{EPA}} \rightarrow qqqq$	4018.7	2420.6
$\gamma_{\text{BS}}\gamma_{\text{BS}} \rightarrow qqqq$	21406.2	13050.3

Table 1.2.: Cross sections of signal and background processes at 1.4 and 3 TeV. In the above table $q \in u, \bar{u}, d, \bar{d}, s, \bar{s}, c, \bar{c}, b$ or \bar{b} while $l \in e^\pm, \mu^\pm$ or τ^\pm and $\nu \in \nu_e, \nu_\mu$ and ν_τ . The subscript EPA or BS for the incoming photons indicate whether the photon is generated from the equivalent photon approximation or beamstrahlung.

operating energy is used to model the energy of the incoming photons. Included in these cases are the photon-photon interactions from photons appearing from the EPA and beamstrahlung processes.

A dominant background process appearing at CLIC is $\gamma\gamma \rightarrow \text{Hadron}$. Example Feynman diagrams for such processes is shown in figure ???. Unlike the majority of other background processes, such as incoherent pair production of e^+e^- pairs from beamstrahlung photons and beam halo muons from interactions of the beam with particles outside the detector, the $\gamma\gamma \rightarrow \text{Hadron}$ processes have a large transverse momentum and cannot be vetoed with a simple transverse momentum cut. To account

for this non negligible background $\gamma\gamma \rightarrow \text{Hadron}$ events are overlayed onto CLIC samples. The number of events overlayed per event is drawn from a Poisson with a mean of 3.2 for 3 TeV and 1.3 for 1.4 TeV samples. Maybe include CDR plot on page 54.

1.8.1. Pre Selection

The primary selection of the $\nu\nu qqqq$ signal will be done using a multivariant analysis, however, in an attempt to veto obvious backgrounds a simple cut based preselection is applied. Cuts are applied to the transverse momentum, invariant mass of the visible system and the number of isolated leptons. The raw distributions of these variables is shown in figures 1.11, 1.12 and 1.13. Based on these distributions the following cuts were applied:

- Transverse momentum > 100 GeV. This cut is effective due to the presence of missing energy in the form of neutrinos in the signal final state.
- Visible mass of the system > 200 GeV. This cut is effective for accounting for the missing energy of the neutrinos in the final state along the longitudinal direction of the detector instead.
- Number of isolated leptons $= 0$. This cut vetos a large number of events with leptons in the final state. The effect of these preselection cuts can be found in table 1.3. While a large fraction of the signal events are lost through these cuts, particularly the transverse momentum cuts, a much large fraction of background events are removed justifying the cut.

1.8.2. MVA

A multivariant analysis is applied to the data set to refine the selection. The following variables were used for training the TMVA selection.

1.9. Fit

Appendix A.

Pointless extras

*“Le savant n’étudie pas la nature parce que cela est utile;
il l’étudie parce qu’il y prend plaisir,
et il y prend plaisir parce qu’elle est belle.”*
— Henri Poincaré, 1854–1912

Appendixes (or should that be “appendices”?) make you look really clever, ‘cos it’s like you had more clever stuff to say than could be fitted into the main bit of your thesis. Yeah. So everyone should have at least three of them...

A.1. Anomalous Gauge Coupling Quartic Vertices Of Relevance in Vector Boson Scattering

The anomalous gauge couplings involving α_4 and α_5 arise in EFT through the addition of the following terms to the Lagrangian.

$$\text{Tr}(V^\mu V_\nu) \text{Tr}(V^\nu V_\mu) \text{ and } [\text{Tr}(V^\mu V_\mu)]^2 \quad (\text{A.1})$$

Where V_μ is defined in the following way.

$$V_\mu = \Sigma(D_\mu \Sigma)^\dagger \quad (\text{A.2})$$

and Σ , the Higgs field matrix, is defined as.

$$\Sigma = \exp\left(-\frac{i}{v}\mathbf{w}\right) \quad (\text{A.3})$$

Where $\mathbf{w} = w^a \sigma^a$. w^a are the ... and σ^a are the Pauli spin matrices. The covariant derivative of the Higgs field matrix is

$$D_\mu \Sigma = (\partial_\mu + \frac{ig}{2}W_\mu - \frac{ig'}{2}B_\mu \sigma^3)\Sigma \quad (\text{A.4})$$

For clarity consider the unitarity gauge where $\mathbf{w} = 0$, which implies $\Sigma = 1$. In this gauge V_μ takes the following form.

$$\begin{aligned} V_\mu &= \frac{i}{2}(gW_\mu^i \sigma^i - g'B_\mu \sigma^3) = \frac{i}{2} \begin{pmatrix} gW_\mu^3 - g'B_\mu & g(W_\mu^1 - iW_\mu^2) \\ g(W_\mu^1 + iW_\mu^2) & -gW_\mu^3 + g'B_\mu \end{pmatrix} \\ &= \frac{i}{2} \begin{pmatrix} \sqrt{g^2 + g'^2}Z_\mu & g\sqrt{2}W_\mu^+ \\ g\sqrt{2}W_\mu^- & \sqrt{g^2 + g'^2}Z_\mu \end{pmatrix} \end{aligned}$$

Where the relationship between the mass and gauge symmetry basis are as follows.

$$W_\mu^+ = \frac{1}{\sqrt{2}}(W_\mu^1 - iW_\mu^2) \quad (\text{A.5})$$

$$W_\mu^- = \frac{1}{\sqrt{2}}(W_\mu^1 + iW_\mu^2) \quad (\text{A.6})$$

$$Z_\mu = c_w W_\mu^3 - s_w B_\mu \quad (\text{A.7})$$

$$A_\mu = s_w W_\mu^3 + c_w B_\mu \quad (\text{A.8})$$

With $c_w = \frac{g}{\sqrt{g^2 + g'^2}}$ and $s_w = \frac{g'}{\sqrt{g^2 + g'^2}}$. Consider the expansion of the terms to be included in the Lagrangian.

$$V^\mu V_\nu = \frac{-1}{4} \begin{pmatrix} \sqrt{g^2 + g'^2} Z^\mu & g\sqrt{2} W^{+\mu} \\ g\sqrt{2} W^{-\mu} & \sqrt{g^2 + g'^2} Z^\mu \end{pmatrix} \begin{pmatrix} \sqrt{g^2 + g'^2} Z_\nu & g\sqrt{2} W_\nu^+ \\ g\sqrt{2} W_\nu^- & \sqrt{g^2 + g'^2} Z_\nu \end{pmatrix} \quad (\text{A.9})$$

$$\text{Tr}[V^\mu V_\nu] = \frac{-1}{2} ((g^2 + g'^2) Z^\mu Z_\nu + g^2 W^{+\mu} W_\nu^- + g^2 W^{-\mu} W_\nu^+) \quad (\text{A.10})$$

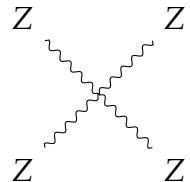
$$\text{Tr}[V^\mu V_\nu] \text{Tr}[V_\mu V^\nu] = \frac{(g^2 + g'^2)^2}{4} (Z^\mu Z_\mu)^2 + g^2 (g^2 + g'^2) (Z^\mu Z^\nu W_\mu^- W_\nu^+) \quad (\text{A.11})$$

$$+ \frac{g^4}{2} (W^{-\mu} W_\mu^+)^2 + \frac{g^4}{2} (W^{-\mu} W^{+\nu} W_\mu^- W_\nu^+) \quad (\text{A.12})$$

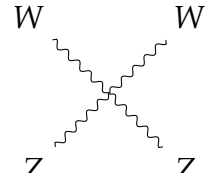
$$\text{Tr}[V^\mu V_\mu]^2 = \frac{(g^2 + g'^2)^2}{4} (Z^\mu Z_\mu)^2 + g^2 (g^2 + g'^2) (Z^\mu Z^\nu W_\mu^- W_\nu^+) \quad (\text{A.13})$$

$$+ g^4 (W^{-\mu} W_\mu^+)^2 \quad (\text{A.14})$$

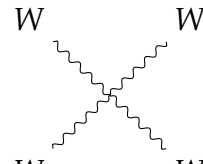
These two terms change the cross section for the vector boson scattering processes at CLIC that involve $ZZ \rightarrow ZZ$, $W^+ W^- \rightarrow ZZ$, $ZZ \rightarrow W^+ W^-$ and $W^+ W^- \rightarrow W^+ W^-$.



$$\subset (\alpha_4 + \alpha_5) \frac{(g^2 + g'^2)^2}{4} \quad (\text{A.15})$$



$$\subset (\alpha_4 + \alpha_5) g^2 (g^2 + g'^2) \quad (\text{A.16})$$



$$\subset (\alpha_4 + 2\alpha_5) \frac{g^4}{2} \text{ and } \frac{g^4}{2} \alpha_4 \quad (\text{A.17})$$

Colophon

This thesis was made in $\text{\LaTeX}2_{\epsilon}$ using the “hepthesis” class [\[2\]](#).

Bibliography

- [1] Toshinori Abe et al. The International Large Detector: Letter of Intent. 2010, 1006.3396.
- [2] Andy Buckley. The hepthesis \LaTeX class.
- [3] Wolfgang Kilian, Thorsten Ohl, and Jurgen Reuter. WHIZARD: Simulating Multi-Particle Processes at LHC and ILC. *Eur. Phys. J.*, C71:1742, 2011, 0708.4233.
- [4] J. S. Marshall, A. MÃijnnich, and M. A. Thomson. Performance of Particle Flow Calorimetry at CLIC. *Nucl. Instrum. Meth.*, A700:153–162, 2013, 1209.4039.
- [5] Mauro Moretti, Thorsten Ohl, and Jurgen Reuter. O’Mega: An Optimizing matrix element generator. 2001, hep-ph/0102195.
- [6] M. A. Thomson. Particle Flow Calorimetry and the PandoraPFA Algorithm. *Nucl. Instrum. Meth.*, A611:25–40, 2009, 0907.3577.

List of figures

1.1. Event weights from Whizard for 1.4TeV $\nu\nu qqqq$ final state events. . . .	4
1.2. Comparison between the invariant mass of the visible system for samples used in this analysis and the official CLIC samples for the $\nu\nu qqqq$ final state.	5
1.3. Comparison between the $\cos\theta_{Missing}$ for samples used in this analysis and the official CLIC samples for the $\nu\nu qqqq$ final state.	5
1.4. Reconstructed invariant masses for different choices of jet algorithm for 1.4 TeV and 3 TeV $\nu\nu qqqq$ events.	8
1.5. χ^2 Sensitivity contours for the $qqqq\nu\nu$ final state arising from a fit to $\cos\theta_{jets}^*$ at 1.4 TeV for different values of the R parameter used in the jet reconstruction.	12
1.6. χ^2 Sensitivity contours for the $qqqq\nu\nu$ final state arising from a fit to $\cos\theta_{jets}^*$ at 1.4 TeV for different PFO selections.	13

List of tables

1.1. Cross section for selected processes for given value of α_4 and α_5	6
--	---